

## Article

# Study on Reactive Air Brazing of p-SiO<sub>2</sub> Ceramic with Ag-xCuO Filler Metal

Yongwei Chen <sup>1</sup>, Qiang Ma <sup>1,2,3,\*</sup> and Peng He <sup>2,\*</sup>

- <sup>1</sup> Key Laboratory of Advanced Welding Technology of Jiangsu Province, Jiangsu University of Science and Technology, Zhenjiang 212003, China; justchenyw@163.com
- <sup>2</sup> State Key Laboratory of Advanced Welding and Joining, Harbin Institute of Technology, Harbin 150001, China
- <sup>3</sup> Zhejiang Seleno Science and Technology Co., Ltd., Jinhua 321016, China
- \* Correspondence: 201900000093@just.edu.cn (Q.M.); hithepeng@hit.edu.cn (P.H.); Tel.: +86-18362882927 (P.H.)

**Abstract:** Reactive air brazing of porous SiO<sub>2</sub> ceramic (p-SiO<sub>2</sub>) was achieved using Ag-CuO filler metal. When brazing p-SiO<sub>2</sub>, two main problems existed. Firstly, the wettability of the Ag filler metal on the surface of p-SiO<sub>2</sub> was poor. Secondly, the residual stress caused by the mismatch of the coefficient of thermal expansion was high in the joint. In order to solve these problems, the effects of CuO contents on the p-SiO<sub>2</sub> brazed joint were analyzed. In a wetting experiment, the addition of CuO significantly improved the wettability of the Ag-CuO/p-SiO<sub>2</sub> system. With the content of CuO increasing, the contact angle decreased from 90° to 0°. In addition, when the content of CuO increased to 0.5 mol%, the contact angle decreased from 90° to 52°. Then, during brazing p-SiO<sub>2</sub> with the Ag-xCuO filler metal, the typical interfacial microstructure of the joints brazed at 1000 °C for 30 min was p-SiO<sub>2</sub> ceramic/Ag (s,s) + SiO<sub>2</sub> + CuO/Ag (s,s)/Ag (s,s) + SiO<sub>2</sub> + CuO/p-SiO<sub>2</sub> ceramic. Meanwhile, Ag-CuO infiltrated into the p-SiO<sub>2</sub> ceramic and an infiltration layer formed. The infiltration layer was composed of Ag (s,s) + SiO<sub>2</sub> + CuO and the infiltration layer was conductive to form a good gradient transition of the coefficient of thermal expansion (CTE). Then, the residual stress in the joint was released and the shear strength improved. In addition, with the content of CuO increasing, the depth of the infiltration layer increased. Furthermore, when the content of CuO was 0.5 mol%, the maximum shear strength of the joint was 55 MPa.

**Keywords:** reactive air brazing; Ag-CuO; wettability; infiltration layer; residual stress



**Citation:** Chen, Y.; Ma, Q.; He, P. Study on Reactive Air Brazing of p-SiO<sub>2</sub> Ceramic with Ag-xCuO Filler Metal. *Metals* **2023**, *13*, 1561. <https://doi.org/10.3390/met13091561>

Academic Editor: Guido Di Bella

Received: 14 July 2023

Revised: 17 August 2023

Accepted: 29 August 2023

Published: 6 September 2023



**Copyright:** © 2023 by the authors. Licensee MDPI, Basel, Switzerland. This article is an open access article distributed under the terms and conditions of the Creative Commons Attribution (CC BY) license (<https://creativecommons.org/licenses/by/4.0/>).

## 1. Introduction

Great attention has been paid to porous ceramic due to its good properties, such as high specific surface area, low thermal conductivity, and density. Furthermore, the advantages of SiO<sub>2</sub> ceramic, such as fracture toughness, thermal stability, and corrosion resistance, have satisfied the demands of the aerospace, optics, bioengineering, and electronics industries [1,2]. It was concluded that the development of porous SiO<sub>2</sub> ceramic (p-SiO<sub>2</sub>) was very important. However, p-SiO<sub>2</sub> was difficult to process into complex structural parts, resulting from its high brittleness and hardness. Therefore, the realization of p-SiO<sub>2</sub>-p-SiO<sub>2</sub> joints was indispensable. In recent years, brazing was regarded as one of the most important methods for jointing ceramic joints [3,4]. The methods of brazing were divided into active metal brazing (AMB) and reactive air brazing (RAB). When using AMB to braze ceramic joints, due to the difficulty in wetting ceramics, active elements were usually added in the filler metal to react with ceramics, such as Ti, Zr, and Cr. Thus, chemical bonding between the ceramic and filler metal was achieved [5–8]. However, the resulting joints were easily oxidized at high temperatures, and the shear strength and hermeticity of joints reduced [9]. High vacuum and inert atmosphere limited the wide application of AMB [10–17], while it was worth noting that the joints brazed using RAB possessed excellent high-temperature oxidation resistance [18,19]. During the RAB process, the oxide compound may react with the surface of the ceramic, newly forming a surface

wetting ceramic. Glass was one of the main filler metals used in RAB, but due to its poor fluidity and high brittleness, pores and cracks easily formed in the joint. Another filler metal was composed of noble metals (Ag, Au, Ag-Pt [20]) and metal oxides ( $\text{Al}_2\text{O}_3$ , CuO [21],  $\text{V}_2\text{O}_5$  [22]). Compared to the above filler metal systems, Ag-CuO was less expensive and could provide better wettability and toughness. During brazing p-SiO<sub>2</sub> and p-SiO<sub>2</sub> (p-SiO<sub>2</sub> joint) with the Ag-CuO filler metal, two major issues existed. Firstly, the wettability of the Ag-CuO/p-SiO<sub>2</sub> system was poor and the shear strength of the joint reduced. Secondly, the high mismatch of the coefficient of thermal expansion (CTE) between the Ag-CuO filler metal and p-SiO<sub>2</sub> resulted in forming residual stress and decreased the shear strength of the joint.

Recently, scholars have carried out some research on Ag-CuO filler metal. For instance, Kati Raju et al. brazed GDC-LSCF ceramics with Ag-10 wt.% CuO paste [23]. The experiment showed that although CuO did not react with ceramic to form an intermediate compound, the wettability of Ag-10 wt.% CuO on the ceramic was adequate. The reason was that a sufficient liquid–solid interaction formed during RAB. Cao et al. brazed YSZ and  $\text{Al}_2\text{O}_3$  using Ag-CuO filler metal through RAB [9]. It was found that the  $\text{Al}_2\text{O}_3$  substrate reacted strongly with the Ag-8 mol% CuO filler metal. A continuous  $\text{CuAl}_2\text{O}_4$  layer and atomic bonding formed at the interface, which improved the wettability of the Ag-CuO/ $\text{Al}_2\text{O}_3$  system. Gui et al. successfully brazed  $\text{Si}_3\text{N}_4$  with itself using Ag-CuO filler metal [24]. It was revealed that the wettability of the Ag-CuO/ $\text{Si}_3\text{N}_4$  system was improved by the  $\text{SiO}_2$  layer. However, due to excessive CuO, cracks and pores formed in the joint. Based on the above research, it can be seen that the wettability and the interfacial reaction of Ag-CuO on ceramic joints have mainly been studied by scholars, while the influence of residual stress has been neglected. At present, the interfacial structure of joints was designed by scholars to relieve residual stress. Sun et al. brazed p- $\text{Si}_3\text{N}_4$  to Invar alloy with Cu-20 wt% Ti filler metal [25]. The investigation showed that a continuous infiltration layer formed in the surface of p- $\text{Si}_3\text{N}_4$ . The infiltration layer was beneficial in terms of improving the shear strength of the joint. Zhao et al. investigated the vacuum brazing of p- $\text{Si}_3\text{N}_4$  ceramic and TiAl alloy with AgCu filler [26]. It was seen that an appropriate thickness of the infiltration layer was beneficial for the formation of a good transition of CTE, relieving residual stress and improving the shear strength of the joint.

Therefore, to achieve a high-quality joint, here, we designed an infiltration layer to assist brazing p-SiO<sub>2</sub> with itself and with Ag-CuO filler metal. The effects of the CuO components on the wettability of the Ag-CuO/p-SiO<sub>2</sub> system were analyzed, and the microstructure and mechanical properties of the p-SiO<sub>2</sub> joint were explored with emphasis. Then, the strengthening mechanism of the p-SiO<sub>2</sub> joint was clarified.

## 2. Experiment Procedures

### 2.1. Sample Preparation

p-SiO<sub>2</sub> ceramics (Shenzhen Haitao Technology Co., Ltd., Shenzhen, China) and cross-sections of joints were cut using an automatic precision cutting machine (Shenyang Kejing Automation Equipment Co., Ltd., Shengyang, China). The shear strength of the p-SiO<sub>2</sub> ceramic was about 60 MPa. The basements were cut into 5 mm × 5 mm × 5 mm pieces and 10 mm × 10 mm × 5 mm pieces for microstructure observation and mechanical testing, respectively. Before wetting and brazing experiments, p-SiO<sub>2</sub> ceramics were polished with 400#, 800#, 1000#, and 1500# sandpaper and then cleaned ultrasonically with alcohol for 15 min. The Ag-xCuO filler metal employed in this study consisted of Ag and CuO powders. Ag powders (purity: 99.9%, average particle size: 5 μm) and CuO powders (purity: 99.9%, average particle size: 5 μm) were purchased from Bisley New Materials (Suzhou) Co., Ltd., Jiangsu, China. Three Ag-xCuO (x = 0, 0.5, 1.0 mol%) powder mixtures were prepared by ball-milling for 1.5 h using a planetary ball miller at a speed of 400 r/min. Then, the mixed powders were heated in a water bath and dried. Subsequently, the Ag-xCuO filler metals were pressed into pieces with dimensions of Ø15 mm × 100 μm using a

tablet press (FW-4, Tianjin Tianguang Optical Instrument Co., Ltd., Tianjin, China) to make it easier to assemble.

## 2.2. Wetting and Brazing Process

During wetting experiments, a vacuum wetting angle measuring instrument (OCA20, Stuttgart, German) was used to measure the contact angle. According to the order in Figure 1a, Ag-xCuO filler metal was sandwiched between two p-SiO<sub>2</sub> ceramic surfaces. Then, the specimens were placed in a muffle furnace for RAB. The brazing process parameters are shown in Figure 1b. Firstly, the specimens were heated to 1000 °C (brazing temperature) at a rate of 10 °C/min, then held for 30 min (brazing time). Finally, in order to decrease the thermal stress generated in the cooling process, the specimens were slowly reduced to room temperature at a rate of 5 °C/min. In addition, a small amount of the Ag-xCuO filler metals was, respectively, placed on the surfaces of p-SiO<sub>2</sub>, then heated with the same parameters to prepare the wetting sample. The shear test of joints is shown in Figure 1c. The shear strength of the brazing joint was the average value of five samples with the same brazing parameters.

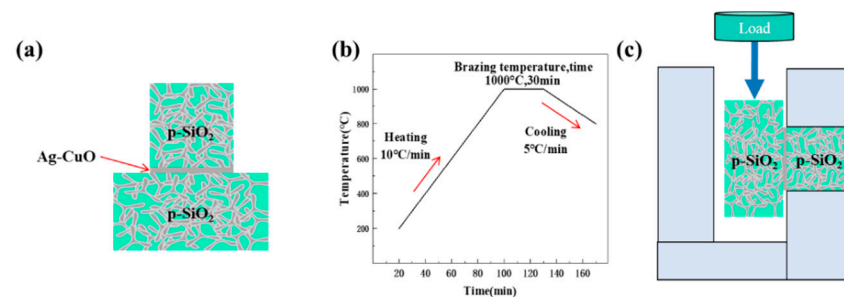


**Figure 1.** The process of brazing p-SiO<sub>2</sub> joint: (a) specimen assembly diagram; (b) brazing process parameters; (c) shear test.

## 2.3. Microstructure Analysis and Property Measurement

The microstructure of the p-SiO<sub>2</sub> joints was analyzed using a scanning electron microscope (SEM, JSM-6480, Akishima, Japan) equipped with an energy-dispersive spectrometer (EDS, INCA Energy 300, Oxfordshire, UK). An X-ray diffractometer (XRD-6000, Shimadzu, Japan) was used to detect the phases in the brazing seam from the angle of 10° to 90° at a rate of 4°/min. The shear strength of joints was tested using an electronic universal testing machine (Instron-1186, Instron, Shanghai, China) at a rate of 0.5 mm/min. After shear testing, the fracture surfaces of the joints were observed using an emission scanning electron microscope (SEM, Helio Nanolab600i, Hillsboro, OR, USA).

## 3. Results and Discussion

### 3.1. The Effect of Content of CuO on the Wettability of Ag-CuO/p-SiO<sub>2</sub> System

The wettability of the Ag-CuO filler metal on the surface of the p-SiO<sub>2</sub> ceramic played a crucial role in determining the brazing joint quality. In this analysis, the effect of the content of CuO on the wettability of Ag-CuO/p-SiO<sub>2</sub> was investigated. The contact angle and wettability of the Ag-xCuO (x = 0, 0.5, 1.0 mol%) filler metals on the surface of p-SiO<sub>2</sub> is shown in Figure 2. It can be seen in Figure 2 that the contact angle showed a significant downward trend with the content of CuO increasing, and with the content of CuO increasing from 0 mol% to 1.0 mol%, the contact angle decreased from 90° to 0°. The wetting area and the decrease rate of the wetting angle gradually increased, and the maximum rate was reached at Ag-1.0 mol% CuO. When the content of CuO was same and the brazing temperature was 1000 °C, with the brazing time increasing, the contact angle first rapidly decreased, then stabilized. In addition, macroscopic morphologies of the contact angle of the Ag-xCuO/p-SiO<sub>2</sub> system are shown in Figure 2. It can be observed that the contact angles of Ag/p-SiO<sub>2</sub>, Ag-0.5 mol% CuO/p-SiO<sub>2</sub>, and Ag-1.0 mol% CuO/p-SiO<sub>2</sub>

were  $90^\circ$ ,  $52^\circ$ , and  $0^\circ$ , respectively. Therefore, it can be inferred that the wettability of Ag-xCuO/p-SiO<sub>2</sub> was significantly improved by the addition of CuO.

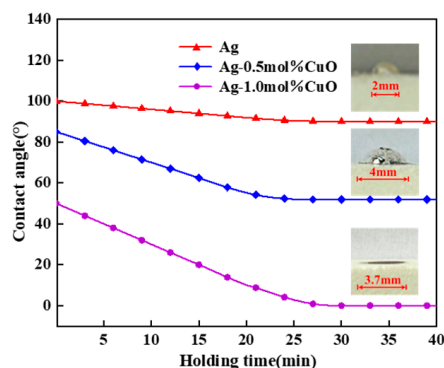


**Figure 2.** Contact angle and macroscopic morphologies of Ag-xCuO wetting on the surface of p-SiO<sub>2</sub>.

Then, in order to further explore the reasons for the improved wettability of the Ag-xCuO/p-SiO<sub>2</sub> system, the microstructure of the Ag-xCuO/p-SiO<sub>2</sub> system was observed. As shown in Figure 3, it can be seen that with the content of CuO increasing, the contact angle of the Ag-xCuO/p-SiO<sub>2</sub> system decreased, and the Ag-xCuO filler metal gradually infiltrated into the surface layer of the p-SiO<sub>2</sub> ceramic. It is worth noting that as shown in Figure 3, it can be seen that due to the large mismatch of CTE between Ag-CuO and p-SiO<sub>2</sub> and the high cooling rate, cracks formed in the cross section. From Figure 3a,b, it can be observed that as the content of CuO increased from 0 to 0.5 mol%, the contact angle of the Ag-CuO/p-SiO<sub>2</sub> system was apparently reduced from  $90^\circ$  to  $52^\circ$ , indicating wettability was improved by the addition of CuO. When the content of CuO was further increased to 1.0 mol%, it was found that the contact angle was nearly  $0^\circ$ , and almost all of the Ag-1.0 mol% CuO infiltrated into the surface layer of the p-SiO<sub>2</sub> ceramic (see Figure 3c). Based on the above discussion, it can be inferred that with the content of CuO increasing, the depth of Ag-CuO filler metal infiltration into the surface layer of p-SiO<sub>2</sub> increased and the contact angle of Ag-CuO/p-SiO<sub>2</sub> decreased. This may be because the surface energy increased with the introduction of CuO. The Ag-CuO filler metal was more hydrophilic and the contact angle of Ag-CuO/p-SiO<sub>2</sub> system reduced, indicating the wettability improved. In addition, the affinity between the surface of p-SiO<sub>2</sub> and CuO was high, which facilitated the Ag-CuO filler metal infiltrating into the surface layer of p-SiO<sub>2</sub>. Then, as the content of CuO increased, the concentration of CuO available for interaction with the p-SiO<sub>2</sub> surface was high and the depth of the infiltration layer increased.

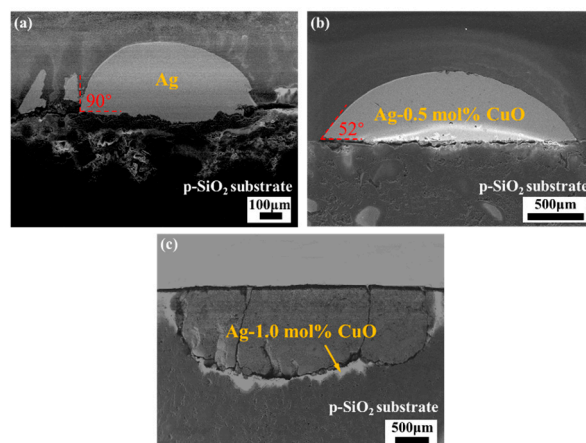


**Figure 3.** Microstructure morphology of Ag-xCuO wetting on the surface of p-SiO<sub>2</sub>: (a) Ag, (b) Ag-0.5 mol% CuO, (c) Ag-1.0 mol% CuO.

### 3.2. The Typical Microstructure of p-SiO<sub>2</sub> Brazed Joints

Understanding the microstructure of a brazing joint was important for evaluating the quality of the p-SiO<sub>2</sub> joint. Thus, the typical microstructure of the p-SiO<sub>2</sub> joint was analyzed. With the brazing temperature of 1000 °C for 30 min, the typical microstructure of p-SiO<sub>2</sub> joint brazed using Ag-0.5 mol% CuO is shown in Figure 4. As shown in Figure 4a, the brazing seam of the p-SiO<sub>2</sub> joint was divided into two regions: Region I (brazing seam center) and Region II (infiltration layer). The enlarged microstructure of Region II is shown in Figure 4b. According to the results of EDS and XRD (see Table 1 and Figure 5), the main composition of points A and B was 87.98 at.% Ag and 78.78 at.% Ag; thus, it can be inferred that the points A and B were Ag. The main composition of point C was 32.69 at.% Si and 63.33 at.% O, and the atomic ration of Si and O was close to 1 to 2. Thus, it can be inferred that the point C was SiO<sub>2</sub> phase. The main composition of point D was 47.65 at.% Cu and 43.33 at.% O, and the atomic ration of Cu and O was close to 1 to 1. Thus, it can be inferred that the point D was CuO phase. In addition, the Ag-0.5 mol% CuO filler metal infiltrated into the surface layer of the p-SiO<sub>2</sub> ceramic and formed Region II. Ag distribution was uniform in Region II. It is worth noting that the CuO phase still existed in the microstructure of the p-SiO<sub>2</sub> joint. This may be because CuO and SiO<sub>2</sub> were both stable compounds and no strong reactivity was exhibited under the brazing condition. Overall, while no typical chemical interaction was exhibited between CuO and SiO<sub>2</sub>, surface phenomena or weak physical interactions may have occurred in this study. Because of the polar nature, the affinity of CuO for the surface of SiO<sub>2</sub> was high, which facilitated the Ag-CuO filler metal to infiltrate into the surface layer of p-SiO<sub>2</sub>. Then, an infiltration layer formed, and the infiltration layer was conducive to form a good gradient transition of CTE. The residual stress of the joint was released, so the shear strength of the joint increased to 55 MPa.

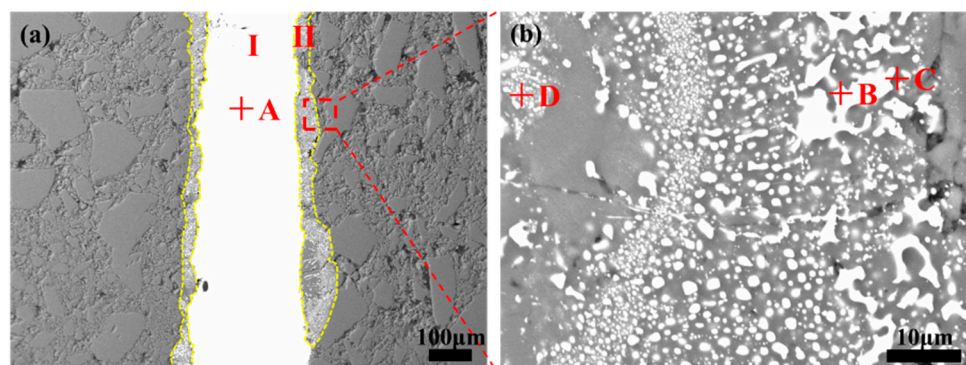


**Figure 4.** Typical microstructure of p-SiO<sub>2</sub> joint brazed using Ag-0.5 mol% CuO: (a) complete microstructure of joint, (b) the amplification of Region II.

**Table 1.** EDS results of p-SiO<sub>2</sub> joint.

Position	Composition (at.%)				Phases
	Ag	Si	Cu	O	
A	87.98	4.35	2.38	5.29	Ag
B	78.78	1.64	0.11	19.47	Ag
C	3.97	32.69	0.01	63.33	SiO <sub>2</sub>
D	4.48	4.54	47.65	43.33	CuO

In order to further investigate the interfacial bonding mechanism between Ag-0.5 mol% CuO and p-SiO<sub>2</sub> ceramic, element line scanning and mapping of the infiltration layer was conducted and is presented in Figure 6. From Figure 6a, it can be seen that the element Ag diffused from the brazing seam to the p-SiO<sub>2</sub> ceramic, and no interaction with p-SiO<sub>2</sub> existed. The element Cu mainly diffused to the surface of the SiO<sub>2</sub> particles because of the physical association between CuO and SiO<sub>2</sub> particles. From Figure 6b–d, it can be seen

that the element Ag was mainly distributed in the pores on the surface of p-SiO<sub>2</sub>. The element Cu was hard to detect, due to its little additive amount. The element Si was mainly distributed in p-SiO<sub>2</sub> ceramic; no diffusion occurred. According to the line scan results and the distribution of the main elements, it can be inferred that Ag was concentrated in the brazing seam center, while SiO<sub>2</sub> and diffused Ag were distributed in the infiltration layer. It is worth noting that the element Cu showed almost no diffusion. This may be because the amount of CuO was too small to be detected.

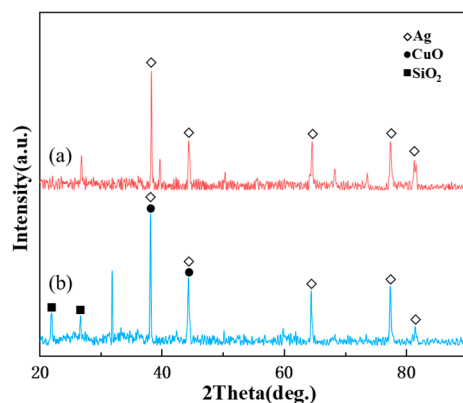


**Figure 5.** XRD pattern of p-SiO<sub>2</sub> joint: (a) close to the brazing seam side, (b) near the p-SiO<sub>2</sub> side.

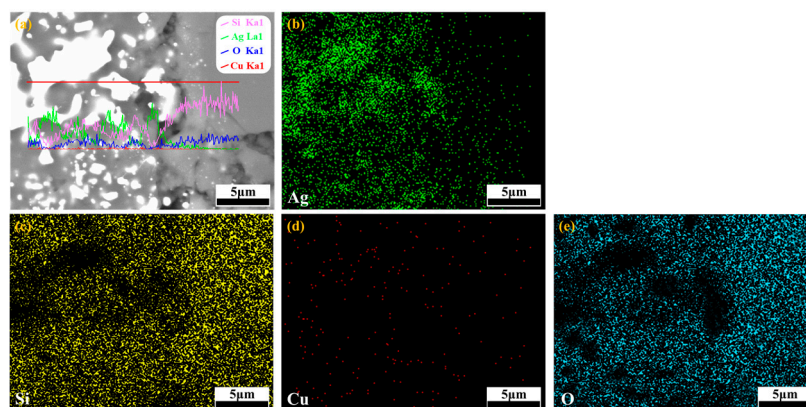


**Figure 6.** Element distribution of p-SiO<sub>2</sub> joint: (a) line scanning results of joints, (b) Ag, (c) Si, (d) Cu, (e) O.

### 3.3. The Effect of CuO Content on the Microstructure and Mechanical Property of p-SiO<sub>2</sub>

The influence of the content of CuO on the microstructure of the p-SiO<sub>2</sub> joint brazed at 1000 °C for 30 min was investigated. Ag, Ag-0.5 mol% CuO, and Ag-1.0 mol% CuO filler metals were used to braze the p-SiO<sub>2</sub> joint, respectively. The microstructure of the p-SiO<sub>2</sub> joint brazed with the Ag-xCuO filler metal is shown in Figure 7. It can be observed that with the content of CuO increasing, the depth of infiltration layer decreased. As shown in Figure 7a, cracks formed in the brazing seam of the p-SiO<sub>2</sub> joint brazed with pure Ag and the width of the brazing seam was 50 μm. This may be because the wettability of Ag on the surface of p-SiO<sub>2</sub> was poor and the mismatch of CTE in the joint was high. The residual stress formed and the shear strength of the joint were only 25 MPa (see Figure 8). When the content of CuO increased to 0.5 mol%, the microstructure of the p-SiO<sub>2</sub> joint was good, without pores and cracks (see Figure 7b), and the width of the brazing seam was 302 μm. It is worth noting that a continuous infiltration layer formed in the brazing seam, and its thickness was 58 μm. Moreover, the shear strength of the joint was further improved to 55 MPa (see Figure 8). While the content of CuO increased to 1.0 mol%, the p-SiO<sub>2</sub> ceramic was filled with Ag(s,s) phase and a small amount of CuO phase, as shown in Figure 7c. No metallurgical bonding formed in the joint and the infiltration layer disappeared, then cracks

formed. Therefore, the shear strength of the joint was reduced to 12 MPa (see Figure 8). Based on the above analysis, it can be inferred that with the content of CuO increasing from 0 mol% to 0.5 mol%, the width of the brazing seam increased, which may be because 1000 °C was higher than the melting point of Ag, so Ag transitioned from a solid to a molten state. The fluidity of Ag was enhanced and the width of the brazing seam decreased. In addition, resulting from the addition of CuO, the binding of Ag-O ionic bonds was promoted, and Ag/O-CuO and Ag/O-SiO<sub>2</sub> interfaces in the infiltration layer formed [24]. Then, the infiltration layer formed in the p-SiO<sub>2</sub> joint, while when the content of CuO further increased to 1.0 mol%, the width of the brazing seam decreased. This may be because as the content of CuO increased, the concentration of CuO available for interaction with the p-SiO<sub>2</sub> surface was improved, and the depth of the infiltration layer increased. Then, the width of brazing seam decreased. Furthermore, because of the infiltration layer forming, a good gradient transition of CTE formed, so the residual stress of the joint was released and the shear strength was increased to 55 MPa.

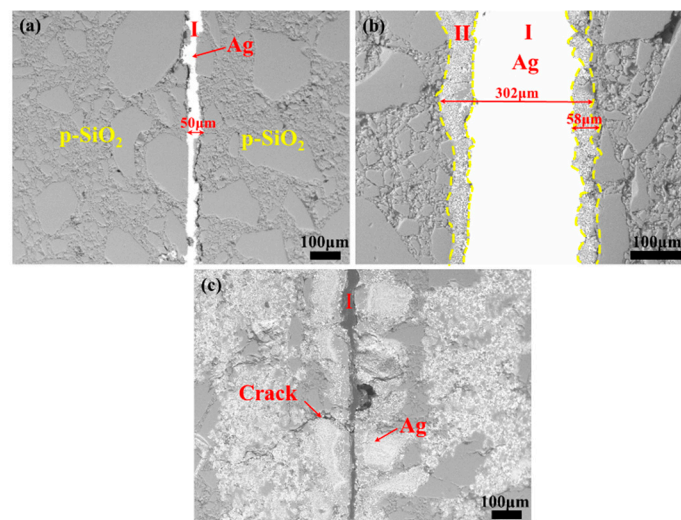


**Figure 7.** Microstructure of p-SiO<sub>2</sub> joint with different CuO contents: (a) Ag, (b) Ag-0.5 mol% CuO, (c) Ag-1.0 mol% CuO. Region I and II as Figure 4.

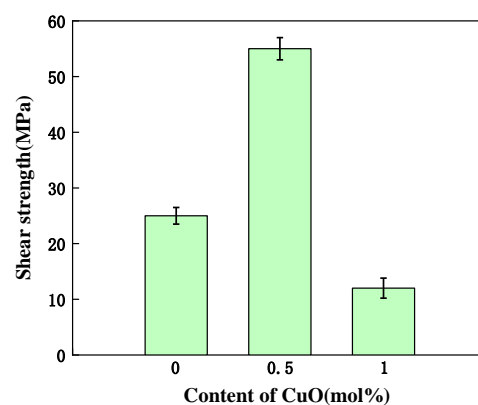


**Figure 8.** Shear strength of p-SiO<sub>2</sub> joints with different CuO contents.

### 3.4. The Interfacial Formation Mechanism of p-SiO<sub>2</sub> Joint

According to the above analysis, a model was established to illustrate the formation mechanism of the p-SiO<sub>2</sub> joint brazed with Ag-CuO in air. As shown in Figure 9, the interfacial mechanism of the joint was clarified. The brazing process was divided into two parts. As shown in Figure 9a, with the brazing temperature increasing to 1000 °C, the Ag-CuO filler metal began to melt and CuO diffused to the surface of the SiO<sub>2</sub> particles. Then,

the surface energy between Ag/p-SiO<sub>2</sub> changed and the Ag-CuO filler metal infiltrated into the surface layer of the p-SiO<sub>2</sub> ceramic, as shown in Figure 9b. Furthermore, due to the addition of CuO, the formation trend of the Ag-O ion bond and interfacial bonding of Ag/O-CuO or Ag/O-SiO<sub>2</sub> were enhanced. Then, with the brazing time extending, Ag-0.5 mol% CuO infiltrated into the surface layer of the p-SiO<sub>2</sub> ceramic and formed a buffer layer composed of Ag, CuO, and SiO<sub>2</sub>. In addition, the infiltration layer was beneficial for forming a good gradient transition of CTE, releasing residual stress and improving the shear strength of the joint.

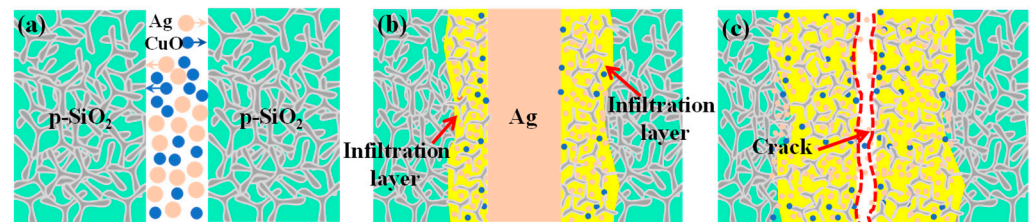


**Figure 9.** Schematic of the p-SiO<sub>2</sub> brazed joint formation mechanism: (a) the Ag-CuO filler metal melting and diffusing stage, (b) the infiltration layer forming, (c) the severe diffusion of Ag-1.0 mol% CuO filler metal.

In order to better understand the strengthening mechanism of p-SiO<sub>2</sub> joints brazed with Ag-CuO filler metal, the microstructure of the fracture surfaces of the p-SiO<sub>2</sub> joints brazed with Ag-xCuO filler metal were investigated and are shown in Figure 10. As shown in Figure 10a, the fracture surface of the joint brazed using the pure Ag filler metal was composed of pores and the p-SiO<sub>2</sub> ceramic. The pores existed in the p-SiO<sub>2</sub> ceramic and the cracks formed in the brazing seam close to the p-SiO<sub>2</sub> ceramic. This may be because the wettability of the Ag filler metal on the surface of the p-SiO<sub>2</sub> ceramic was poor and metallurgical bonding was weak, so cracks formed at the interface of Ag/p-SiO<sub>2</sub>. Therefore, the shear strength of the p-SiO<sub>2</sub> joint brazed with the Ag filler metal was low. The fracture surfaces of the p-SiO<sub>2</sub> joint brazed with Ag-xCuO were the same, and the typical fracture was analyzed. Figure 10b displays the fracture surface of the joint with the content of CuO increased to 0.5 mol%. It seems that the fracture surface of the p-SiO<sub>2</sub> joint brazed with Ag-0.5 mol% CuO was composed of the Ag-0.5 mol% CuO filler metal and p-SiO<sub>2</sub> ceramic. Thus, it can be inferred that cracks formed on the infiltration layer. In other words, the interface strength and wettability of Ag-0.5 mol% CuO/p-SiO<sub>2</sub> were fine during the brazing process, with no cracks or pores occurring at the interface. Therefore, the shear strength of the joints was effectively improved. It is well known that grain boundary strengthening is an important method to impede crack propagation and improve the mechanical property of joints [27–35]. In addition, for p-SiO<sub>2</sub> joints brazed with the Ag-1.0 mol% CuO filler metal, the fluidity of the filler metal was improved and all the filler metal infiltrated into the p-SiO<sub>2</sub> ceramic, as shown in Figure 10c. No metallurgical bonding formed with the p-SiO<sub>2</sub> ceramic, then fracture occurred in the brazing seam. Based on the above analysis, it can be inferred that because of the addition of CuO to the system, the surface energy of the infiltration layer increased, and the hydrophilicity of Ag-CuO/p-SiO<sub>2</sub> improved. The formation trend of the Ag-O ion bond and interfacial bonding of Ag/O-CuO or Ag/O-SiO<sub>2</sub> were enhanced. Then, the Ag-CuO filler metal infiltrated into the surface layer of the p-SiO<sub>2</sub> ceramic and formed an infiltration layer mainly composed of Ag (s,s), CuO, and SiO<sub>2</sub>. Therefore, the residual stress of the p-SiO<sub>2</sub> joints was released and the shear strength of the joints was increased. In summary, it was critical to use the Ag-xCuO filler metal with the proper content of CuO to promote the formation of the infiltration layer, while the good wettability of the Ag-xCuO/p-SiO<sub>2</sub> system was maintained.

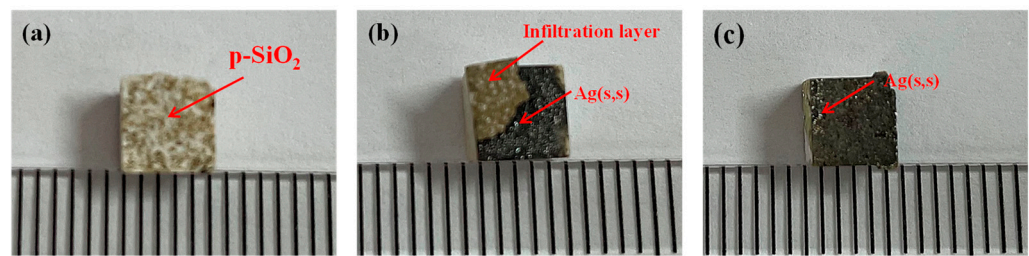


**Figure 10.** Fracture morphology diagram of p-SiO<sub>2</sub> joints brazed using different Ag-xCuO filler metals: (a) Ag; (b) Ag-0.5 mol% CuO; (c) Ag-1.0 mol% CuO.

#### 4. Conclusions

In this work, p-SiO<sub>2</sub> joints were successfully brazed using Ag-CuO filler metal. The effect of the content of CuO on the wettability of the Ag-CuO/p-SiO<sub>2</sub> system and the interfacial microstructure and mechanical property of the p-SiO<sub>2</sub> joint were systematically investigated. The conclusions obtained were as follows:

- (1) With the content of CuO increasing from 0 mol% to 0.5 mol%, the surface energy between the Ag-CuO filler metal and p-SiO<sub>2</sub> ceramic was increased. The wetting angle of the Ag-CuO/p-SiO<sub>2</sub> system decreased from 90° to 52°, and the wettability was greatly improved. When the content of CuO increased to 1.0 mol%, Ag-CuO completely infiltrated into the surface layer of the p-SiO<sub>2</sub> ceramic and the wetting angle was reduced to 0°.
- (2) The typical microstructure of the p-SiO<sub>2</sub> joint brazed using Ag-0.5 mol% CuO at 1000 °C for 30 min was p-SiO<sub>2</sub>/Ag (s,s) + SiO<sub>2</sub> + CuO/Ag (s,s)/Ag (s,s) + SiO<sub>2</sub> + CuO/P-SiO<sub>2</sub>. The infiltration layer was composed of Ag (s,s) + SiO<sub>2</sub> + CuO. In addition, the infiltration layer was conducive to forming a good gradient transition of CTE, releasing the residual stress in the joint, and improving the shear strength of the joint.
- (3) When the p-SiO<sub>2</sub> joint was brazed with the Ag filler metal, the fracture was formed in the brazing seam close to the p-SiO<sub>2</sub> ceramic, and when the joint was brazed with the Ag-xCuO filler metal, the fracture was formed in the infiltration layer. Furthermore, the shear strength of the joint increased first and then decreased with the content of CuO increasing. When the content of CuO was 0.5 mol%, the maximum shear strength of the joint was 55 MPa.

**Author Contributions:** Q.M. supervised the experiment and wrote the paper, Y.C. carried out the experiment, and P.H. instructed in the experimental scheme. All authors have read and agreed to the published version of the manuscript.

**Funding:** This project is supported by the National Natural Science Foundation of China (Grant NO.52105350), State Key Laboratory of Advanced Welding and Joining (AWJ-23R01).

**Institutional Review Board Statement:** Not applicable.

**Informed Consent Statement:** Not applicable.

**Data Availability Statement:** Not applicable.

**Conflicts of Interest:** The authors declare no conflict of interest.

#### References

1. Bian, H.; Song, Y.; Liu, D.; Lei, Y.; Song, X.; Cao, J. Joining of SiO<sub>2</sub> ceramic and TC4 alloy by nanoparticles modified brazing filler metal. *Chin. J. Aeronaut.* **2020**, *33*, 383–390. [\[CrossRef\]](#)
2. Holland, W.; Rheinberger, V.; Apel, E.; Hoen, C.V.T. Principles and phenomena of bioengineering with glass-ceramics for dental restoration. *J. Eur. Ceram. Soc.* **2017**, *27*, 1521–1526. [\[CrossRef\]](#)
3. Wang, Z.; Li, C.; Si, X.; Wu, C.; Qi, J.; Feng, J.; Cao, J. Interfacial microstructure and mechanical properties of SiC joints achieved by reactive air brazing using Ag-V<sub>2</sub>O<sub>5</sub> filler. *J. Eur. Ceram. Soc.* **2019**, *39*, 2617–2625. [\[CrossRef\]](#)

4. Zhao, W.Q.; Zhang, S.Y.; Yang, J.; Lin, T.S.; Dusan, P.S.; He, P. Wetting and brazing of YIG ceramics using Ag–CuO–TiO<sub>2</sub> metal filler. *J. Mater. Res. Technol.* **2021**, *10*, 1158–1168. [[CrossRef](#)]
5. Lin, K.-L.; Singh, M.; Asthana, R. Interfacial characterization of YSZ-to-steel joints with Ag–Cu–Pd interlayers for solid oxide fuel cell applications. *Ceram. Int.* **2012**, *38*, 1991–1998. [[CrossRef](#)]
6. Lin, K.L.; Singh, M.; Asthana, R. Effect of short-term aging on interfacial and mechanical properties of yttria stabilized zirconia (YSZ)/stainless steel joints. *J. Eur. Ceram. Soc.* **2015**, *35*, 1041–1053. [[CrossRef](#)]
7. Hanson, W.B.; Ironside, K.I.; Fernie, J.A. Active metal brazing of zirconia. *Acta Mater.* **2000**, *48*, 4673–4676. [[CrossRef](#)]
8. Wang, D.; Cao, J.; Li, W.; Dai, X.; Feng, J. Zr hydrogenation by cathodic charging and its application in TC4 alloy diffusion bonding. *Int. J. Hydrogen Energy* **2016**, *42*, 6350–6359. [[CrossRef](#)]
9. Cao, J.; Si, X.; Li, W.; Song, X.; Feng, J. Reactive air brazing of YSZ-electrolyte and Al<sub>2</sub>O<sub>3</sub>-substrate for gas sensor sealing: Interfacial microstructure and mechanical properties. *Int. J. Hydrogen Energy* **2017**, *42*, 10683–10694. [[CrossRef](#)]
10. Chao, C.L.; Chu, C.L.; Fuh, Y.K.; Hsu, R.Q.; Lee, S.; Cheng, Y.N. Interfacial characterization of nickel-yttria-stabilized zirconia cermet anode/interconnect joints with Ag-Pd-Ga active filler for use in solid-oxide fuel cells. *Int. J. Hydrogen Energy* **2015**, *40*, 1523–1533. [[CrossRef](#)]
11. Xu, J.C.; Wu, M.F.; Pu, J.; Xue, S.B.; Han, Y.L. Effect of Ca element on oxygen content, wetting and spreading properties of Au–Ga filler metal. *Vacuum* **2020**, *177*, 109380. [[CrossRef](#)]
12. Ma, Q.; Pu, J.; Li, S.G.; Chen, Y.W.; He, P. Introducing a 3D-SiO<sub>2</sub>-fiber interlayer for brazing SiC with TC4 by AgCuTi. *J. Adv. Join. Process.* **2022**, *5*, 100082. [[CrossRef](#)]
13. Xia, C.; Sun, W.; Zhou, Y.; Zhao, M. Effect of Ni-Ti filler on brazed W-Cu/18-8 joints. *J. Mater. Process. Technol.* **2018**, *259*, 15–22. [[CrossRef](#)]
14. Yang, H.; Si, X.; Li, C.; Cao, J. Reactive Air Brazing of TiAl Alloy Using Ag–CuO: Microstructure and Joint Properties. *Crystals* **2021**, *11*, 1496. [[CrossRef](#)]
15. Sharma, A.; Ahn, B. Vacuum brazing of Al<sub>2</sub>O<sub>3</sub> and 3D printed Ti6Al4V lap-joints using high entropy driven AlZnCuFeSi filler. *Sci. Rep.* **2021**, *11*, 9345. [[CrossRef](#)]
16. Sharma, A.; Lee, S.J.; Oh, J.H.; Jung, J.P. AISI 304 Steel Brazing Using A Flexible Brazing Foil Fabricated by Tape Casting Method. *J. Korean Inst. Met. Mater.* **2017**, *55*, 836–844.
17. Sharma, A.; Chae, M.J.; Ahn, B. Brazeability and Microstructure of Ag-28Cu Microjoining Filler Produced by High Energy Ball Milling. *Arch. Met. Mater.* **2020**, *65*, 1323–1327. [[CrossRef](#)]
18. Tucker, M.C.; Jacobson, C.P.; De Jonghe, L.C.; Visco, S.J. A braze system for sealing metal-supported solid oxide fuel cells. *J. Power Sources* **2006**, *160*, 1049–1057. [[CrossRef](#)]
19. Sofie, S.W.; Gannon, P.; Gorokhovskiy, V. Silver–chromium oxide interactions in SOFC environments. *J. Power Sources* **2009**, *191*, 465–472. [[CrossRef](#)]
20. Luo, Y.; Song, X.G.; Hu, S.P.; Xu, Z.Q.; Li, Z.H.; Lei, Y. Reactive air brazing of Al<sub>2</sub>O<sub>3</sub> ceramic with Ag–CuO–Pt composite fillers: Microstructure and joint properties. *J. Eur. Ceram. Soc.* **2021**, *41*, 1407–1414. [[CrossRef](#)]
21. Kim, M.D.; Muhamad, W.; Raju, K.; Kim, S.; Yu, J.H.; Park, C.D.; Yoon, D.H. Efficacy of Ag–CuO filler tape for the reactive air brazing of ceramic–metal joints. *J. Korean Ceram. Soc.* **2018**, *55*, 492–497. [[CrossRef](#)]
22. Sinnamon, K.E.; Meier, A.M.; Joshi, V.V. Wetting and Mechanical Performance of Zirconia Brazed with Silver/Copper Oxide and Silver/Vanadium Oxide Alloys. *Adv. Eng. Mater.* **2014**, *16*, 1482–1489. [[CrossRef](#)]
23. Raju, K.; Muksin; Yoon, D.-H. Reactive air brazing of GDC–LSCF ceramics using Ag–10 wt% CuO paste for oxygen transport membrane applications. *Ceram. Int.* **2016**, *42*, 16392–16395. [[CrossRef](#)]
24. Gui, X.Y.; Zhang, M.F.; Xu, P.H. Experimental and theoretical study on air reaction wetting and brazing of Si<sub>3</sub>N<sub>4</sub> ceramic by Ag–CuO filler metal: Performance and interfacial behavior. *J. Eur. Ceram. Soc.* **2022**, *42*, 432–441. [[CrossRef](#)]
25. Sun, L.; Wei, Q.; Fang, J.; Liu, C.; Zhang, J. Brazing of porous Si<sub>3</sub>N<sub>4</sub> ceramic to Invar alloy with a novel Cu–Ti filler alloy: Microstructure and mechanical properties. *Ceram. Int.* **2020**, *47*, 2068–2076. [[CrossRef](#)]
26. Zhao, Y.; Song, X.; Hu, S.; Zhang, J.; Cao, J.; Fu, W.; Feng, J. Interfacial microstructure and mechanical properties of porous-Si<sub>3</sub>N<sub>4</sub> ceramic and TiAl alloy joints vacuum brazed with AgCu filler. *Ceram. Int.* **2017**, *43*, 9738–9745. [[CrossRef](#)]
27. Lin, H.; Hua, P.; Huang, K.; Li, Q.; Sun, Q. Grain boundary and dislocation strengthening of nanocrystalline NiTi for stable elastocaloric cooling. *Scr. Mater.* **2023**, *226*, 115227. [[CrossRef](#)]
28. Kim, S.E.; Verma, N.; Özerinç, S.; Jana, S.; Das, S.; Bellon, P.; Averbach, R. Strengthening of nanocrystalline Al using grain boundary solute additions: Effects of thermal annealing and ion irradiation. *Materialia* **2022**, *26*, 101564. [[CrossRef](#)]
29. Shu, M.; Zhou, Q.; Shen, Y.; Zhou, Z.; Wang, P.; Chen, L.; Sun, Y.; Xiao, J. Improved creep resistance of 20Cr25NiNb heat resistant steels through grain boundary intermetallic precipitation strengthening. *J. Mater. Res. Technol.* **2023**, *25*, 3728–3743. [[CrossRef](#)]
30. Hu, W.; He, J.; Yang, Z.; Tan, J.; Chen, S.; Liu, S.; Ma, Z.; Liu, Y. Strengthening the grain boundary of Mo alloy via little TiC addition. *Mater. Charact.* **2023**, *203*, 113063. [[CrossRef](#)]
31. He, T.; Qi, Y.; Ji, Y.; Feng, M. Grain boundary segregation-induced strengthening-weakening transition and its ideal maximum strength in nanopolycrystalline FeNiCrCoCu high-entropy alloys. *Int. J. Mech. Sci.* **2023**, *238*, 107828. [[CrossRef](#)]
32. Bai, Y.B.; Zhang, R.; Cui, C.; Zhou, Y.; Sun, X.F. Eliminating embrittlement of GH4065A superalloy at inter-mediate temperature by a novel grain boundary strengthening mechanism. *Mater. Lett.* **2023**, *335*, 133798. [[CrossRef](#)]

33. Guan, B.; Xin, Y.; Huang, X.; Liu, C.; Wu, P.; Liu, Q. The mechanism for an orientation dependence of grain boundary strengthening in pure titanium. *Int. J. Plast.* **2022**, *153*, 103276. [[CrossRef](#)]
34. Lin, X.P.; Dang, Y.Z.; Dai, P.L.; Fang, D.R.; Xu, C.; Wen, B. Microstructure control and strengthening mechanism of fine-grained cast Mg alloys based on grain boundary segregation of Al solute. *Mater. Sci. Eng. A* **2022**, *851*, 143665. [[CrossRef](#)]
35. Lee, S.J.; Sharma, A.; Jung, D.H.; Jung, J.P. Influence of Arc Brazing Parameters on Microstructure and Joint Properties of Electro-Galvanized Steel. *Metals* **2019**, *9*, 1006. [[CrossRef](#)]

**Disclaimer/Publisher's Note:** The statements, opinions and data contained in all publications are solely those of the individual author(s) and contributor(s) and not of MDPI and/or the editor(s). MDPI and/or the editor(s) disclaim responsibility for any injury to people or property resulting from any ideas, methods, instructions or products referred to in the content.